The data were automatically plotted by an X-Y recorder, with the ram pressure along one axis and the displacement of the piston along the other (fig. 2). The bismuth transitions are indicated by a large piston displacement with little change in pressure. When the quartz made contact with the piston the ram pressure increased much more rapidly than in the normal transition in a sample containing only bismuth (fig. 2). In most of the experiments the quartz failed with a loud report, and the records show a rapid decrease of pressure and increase of piston displacement at the time of failure. After rupture, the sample was unloaded, rapidly in some experiments and slowly in others. In three experiments, the sample was unloaded when the axial load was just below the rupture point, as determined in earlier experiments. These samples were sectioned as the others were (see below) for comparison with the ruptured samples.

Because of high (and undetermined) friction between the piston and packings and the pressure vessel in the experiments, and the small but finite strengths of the bismuth and copper in the assembly, the strengths of the samples were not computed directly from the curves. Instead, calibration runs were made using samples of exactly the same geometry as those for quartz experiments, but in which the quartz cylinder was replaced by one of a material with low strength. Indium was chosen as its strength at these pressures (approximately 0.5 kb) is negligible compared with that of quartz and its compressibility is almost identical with that of quartz. In the idealized curves in figure 2, the vertical distance (AB) between the rupture point (A) for a quartz sample and the point (B) on the curve for the calibration run is proportional to the strength of the quartz, minus the load supported by a similar sample of indium under the same conditions. The axial stress on the quartz can be computed from the ram pressure, since the cross-sectional area of the ram and the initial cross-sectional area of the quartz cylinder are known. The accuracy of the Heise-Bourdon gauge used to measure the pressure behind the ram is stated

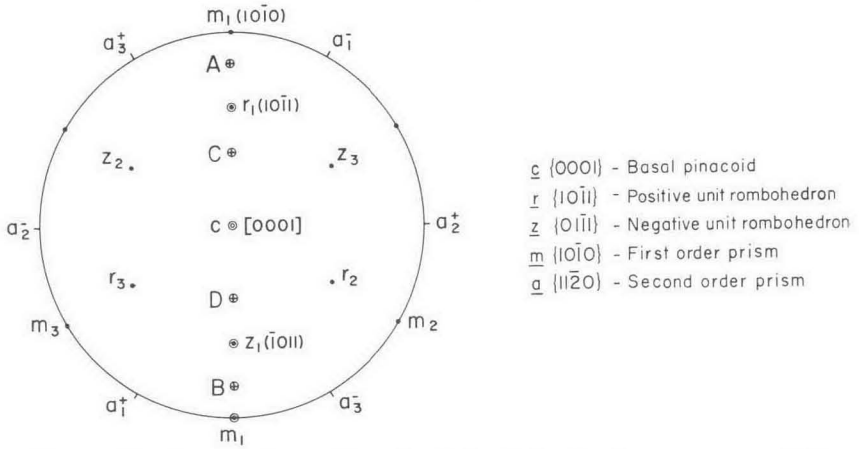

Fig. 3. Equal-area projection (lower hemisphere) showing the common crystal planes of quartz and the convention regarding polarity of the *a*-axes. Directions in which samples were cored are represented by circles.

to be ± 0.5 bars. In converting the ram pressure to axial load on the quartz cylinder, this is equivalent to approximately ± 0.5 kb axial stress on the quartz; this is therefore the precision with which the measurements were made. Since the correction for the strength of indium was approximately the same as the estimated precision of the measurements, no correction was made for this. Changes in the cross-sectional area of the quartz sample due to (1) compressibility of the quartz and (2) elastic distortion of the sample under load are of opposite sign and cancel each other within the precision of the measurements.

The average strain-rate in the quartz during loading was 3×10^{-4} per second. The samples that were deformed but not ruptured showed no macroscopic evidence of deformation. Thus most of the permanent strain in the other samples must have been produced almost instantaneously at rupture, and the deformation before rupture was therefore predominantly elastic.

Preparation of samples and thin sections.—The deformed samples were to be examined optically in thin section, and since it is impossible to determine the orientation of the *a*-axes optically, it was necessary to devise a method of coring and marking the samples so that the orientation of the cylinders, and ultimately the thin sections, would be fully known.

The cylinders were cored from large optical-quality quartz crystals using a diamond-impregnated coring drill. Large crystals with well-developed prism and rhombohedral faces were etched lightly with 40 percent hydrofluoric acid. The shapes of the etch-pits on these faces were used (Ichikawa, 1915) to dis-

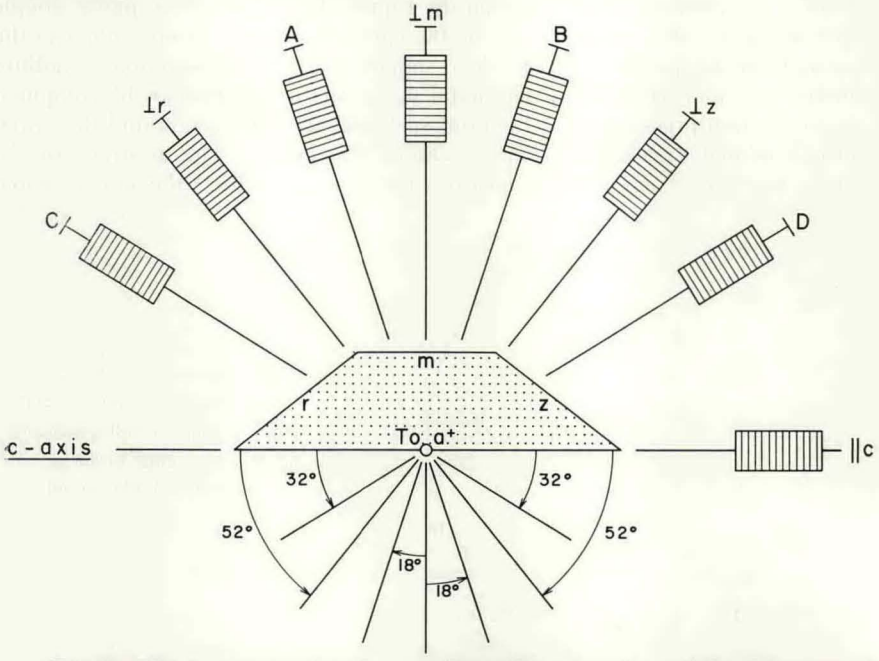

Fig. 4. Diagram representing the crystallographic orientations of the eight types of samples used in the experiments. The crystal is viewed towards the positive end of an *a*-axis.